

Introduction

The increasing resistance of malarial parasites to the existing antimalarial drugs, and in particular of *Plasmodium falciparum* (Pf), has focused efforts towards the discovery of more selective and potent drugs.¹ Hemoglobin(Hb)-degrading enzymes of Pf, emerge as very promising chemotherapeutic targets, because Hb degradation is an unique and critical process for Pf.^{1,2} Up to date, Hb degradation is catalyzed by the concerted action of aspartyl-,³ cysteine-,⁴ metallo-,⁵ and a dipeptidyl amino peptidases⁶ within the digestive vacuole (DV) of the parasite.⁷ Earlier studies indicated that the aspartic proteases plasmepsins (Plms) play essential roles in Pf life cycle, due to the effectiveness of Plms inhibitors abolishing Hb degradation, erythrocyte rupture and parasite development.^{1,8} However, the redundant functional role of these enzymes in Hb digestion has been demonstrated by Plm deletion.^{9,10} This feature indicated that more effective drugs may be only obtained by blocking all Plms.¹¹

Plasmodium falciparum PlmII has been the most extensively characterized of these enzymes with several crystal structures determined,^{12, 13, 14, 15} and potent inhibitors developed.^{16, 17} Approaches used in PlmII structure-based ligand design usually include some popular docking algorithms,^{18, 19, 20, 21, 22; 23, 22} to predict conformations of inhibitor complexes, followed by a method to estimate the binding affinity.¹⁷ However, most of the PlmII inhibitors obtained using these methods have generally shown a limited selectivity towards the human related protease Cathepsin D (hCatD).²⁴ On the other hand, the high degree of structural flexibility of the PlmII active site cavity^{25, 26} allows the accommodation of different inhibitors scaffolds,^{12, 13, 14, 15} which is a notable drawback for drug design using the traditional rigid docking approaches.

What is the consequence of this statement?
single statement without clear relation to rest of the paragraph

Synthetic peptide combinatorial libraries have been used to determine the substrate preference of malarial enzymes in the aspartic protease family.²⁷ An early study of Westling and coworkers suggested the major role of the S3 subsite pocket in the PlmII specificity, based on the higher differences in the kinetic parameters obtained by the amino acid variation in the substrate P3 position.²⁸ These authors found that PlmII prefers large hydrophobic residues within the S3 subsite pocket, while K or D substitutions in P3 were not well tolerated.²⁸ Conversely, the S3 subsite of the hCatD is a hydrophilic and a hydrophobic pocket and indeed, it has been shown that M, I, S and T are the preferred P3 residues for the human enzyme, with the hydrophilic residues binding to the Q14 side chain and the hydrophobic residues binding to hydrophobic amino acids of this pocket.²⁹ It should be noted that the replacement of the M15

Explain this pocket. Maybe figure

why Q14

Picture + maybe move into on pocket?

(thus so, M15 in PlmII is same position as Q14 in hCatD)

(according to the PlmII numbering scheme) by the Q14 (according to the hCatD numbering scheme) is one of the most important differences between the S3 pocket residues of the parasite and the human protein, respectively. ²⁶ However, the thermodynamic effect of the changes in the P3 position of well known PlmII substrates have not been studied by free energy calculations from atomic level simulations. ^{So, how is it studied?}

Among the simulation protocols that aim at calculating free energy differences, perturbation approaches, ^{30, 31, 32} have grown in popularity over the last years. In these protocols the Hamiltonian H is coupled to a parameter λ which is used to drive a system from a state A ($\lambda = 0$) to a state B ($\lambda = 1$). Free energy differences between both states can be computed by equilibrium methods such as free energy perturbation ³³ or thermodynamic integration, ³⁴ or non-equilibrium methods such as those based on the work of Jarzynski, ^{35, 36} and Crooks. ³⁷ Recently, Goette and Grubmuller showed that non-equilibrium methods outperformed the traditional equilibrium methods for test systems that include: *i*) the interconversion of ethane into methanol, *ii*) the switching from ($W \rightarrow G$) in a tripeptide, and *iii*) the binding of two different ligands to the globular protein snuportin 1. ³⁸ Based on their results, they proposed a new non-equilibrium free energy method, termed the Crooks Gaussian Intersection (CGI), which combines the advantages of the available methods (see reference 38 for more details). This method has been used successfully to calculate the thermodynamic stability differences for 109 mutations in the microbial Ribonuclease Barnase. ³⁹ Thus, the questions here are: *i*) can the CGI method be suitable applied to study the binding free energy differences of substitutions in the substrate P3 position over the PlmII substrate affinities?, and *ii*) What can we learn for these calculations for the PlmII inhibitor design process?

In this paper, we presented a detailed analysis of the free energy calculations with the CGI method of PlmII in complex with synthetic chromogenic substrates, to gain a better understanding of the preference of PlmII by large hydrophobic residues within the S3 subsite pocket. ²⁸ Our results agreed with the experimental trend of K_m values of PlmII with the assessed substrates. We also predicted the protonation state of the substrate P3 ionizable residues in the experimental assays. Finally, we showed the differential contributions of the enthalpic and entropic energy terms to the relative binding free energy differences of the changes from $F \rightarrow K^+$, and $F \rightarrow D^0$.

too much detail

as was it studied? why do you want to? K_m is thermodynamic

I hope that is not a question!

too obvious. We always want to learn something.

My opinion! no results is introduced only what you investigated and how.

Results

Analysis of PlmII:Substrate S3 subsite interactions

To better understand the known preference by hydrophobic residues of the PlmII S3 subsite pocket, ~~we calculated 3D models~~ of the PlmII:Substrate complexes. ^{predicted/ simulated for x ns}

Not clear from the figure to me
~~Interestingly,~~ we observed that the P3 position of the substrate was always solvent exposed (Figure 1). In addition, the analysis of the fraction of non-polar/polar contacts between each substrate P3 residue and the PlmII S3 subsite residues (Table I) showed that this rough parameter was not useful to explain the differences in the Michaelis constant values (K_m) taken from the Westling and coworkers study.²⁸ *What is this exactly? why this statement.*

Alchemy free energy calculations *different P3 residues on PlmII binding we*
To analyse the different binding constants between residues
Experimental binding free energy differences $\Delta\Delta G_{\text{exp}}$ for P3 changes were calculated from the Michaelis constant values (K_m).²⁸ *calculated free energy differences.*
The calculated binding free energy differences $\Delta\Delta G_{\text{calc}}$ were determined according to $\Delta G_4 - \Delta G_1$ (Figure 2). *This was done according to FE cycle in figure 2.*
Therefore, changes in the P3 position of the substrate ($A \rightarrow B$) that increases the affinity for the protein have a negative $\Delta\Delta G$, while changes that decrease the affinity have a positive $\Delta\Delta G$. *To test the accuracy As a quick check we calculated compared to exp. values obtained from K_m .²⁸*

We reproduced the experimental trend of binding free differences for the changes in the P3 position of PlmII:Substrates complexes using the CGI method (Table II, Figure 3). *rather see a attraction, because the you also know the size of the data set.*
As result, we obtained a Pearson product-moment correlation $r = 0.5$, with a mean absolute error ($\langle \text{error} \rangle = 4.00 \text{ kJ/mol}$, and a (60%) of the calculated free energy differences within $\pm 4.18 \text{ kJ/mol}$ of the experimental values (Figure 3A). In addition, we observed that the lysine and aspartic acid residues must be in the protonated form in the experimental assays (Table II). *discussion.*
~~It should be noted that~~ taking in to account only the

$\Delta\Delta G_{\text{calc}}$ from the protonation state of the ionizable residues that fit better with experimental $\Delta\Delta G_{\text{exp}}$ values, we obtained a correlation $r = 0.75$, with a mean absolute error ($\langle \text{error} \rangle = 2.58 \text{ kJ/mol}$, and a 78% of the calculated free energy differences within $\pm 4.18 \text{ kJ/mol}$ of the experimental values (Figure 3B).

To better understand the effect from changes in the P3 position over the PlmII:Substrates complexes affinity differences $\Delta\Delta G_{\text{calc}}$, *analysed individual mutation for in the complex (bound) and in solution (unbound)* we calculated the free energy differences $\Delta\Delta G$ in the bound and unbound simulation states (Table II). As can be seen, the change from $F \rightarrow I$ increase the affinity of PlmII for the substrate due to a higher unfavorable effect in the unbound system than in the complex system. Conversely, the P3 changes from F to small hydrophobic (A), neutral polar (S, and D^0) or charged

residues (K^+ , and R) decrease the affinity of Plasmepsin II for the substrate. In this respect, our calculations show that this net effect is observed due to different consequences. The decrease in the affinity for the changes from $F \rightarrow A$, and $F \rightarrow K^+$ is caused by a higher unfavorable effect on the bound state than in the unbound state. On the contrary, the changes from $F \rightarrow S$, and $F \rightarrow D^0$ decrease the PlmII affinity for the substrate due to the lower favorable effect of these mutations on the complex system than in the solvent system. It should be noted that the decrease in the Plasmepsin II affinity for the change from $F \rightarrow R$ is the combination of an unfavorable effect in the complex with a favorable effect in the solvent system. Interesting, our calculations predict that the change for $F \rightarrow Y$ has a null effect over the PlmII:Substrate affinity thanks to a similar compensatory favorable effect in the complex and solvent systems. We have to remark that the P3 changes from other hydrophobic residues (I or A) to neutral polar (S, and D^0) or charged residues (K^+) decrease the affinity of Plasmepsin II for the substrate in a comparable fashion to the F mutation series. On the other hand, our calculations shown that the PlmII has a better affinity for neutral polar residues (S, and D^0) than for positive charge residue (K^+) because of a bigger favorable effect of the mutation on the complex system than on the solvent system.

Entropy and enthalpy calculations *To determine the enthalpic driving force*

To gain a better insight of the effect from the changes in the substrate P3 position over the PlmII:Substrates complexes affinities, we calculated the entropic and enthalpy contributions (Table III) to the binding free energy differences ($\Delta\Delta G_{calc}$), of the F mutations series, using the finite difference relationship of changes in the $\Delta S(T)$ with changes in the $\Delta G(T + \Delta T)$ and $\Delta G(T - \Delta T)$ (see equation 4, 5, and Table I of Supplementary Information). According to our calculations the change from $F \rightarrow I$ increase the affinity of PlmII for the substrate due to the raise in the entropy ($T\Delta\Delta S$) prevails over the enthalpy penalty ($\Delta\Delta H$). It should be noted that this mutation ($F \rightarrow I$) is an entropy driven process due to the combination of the enlarge in the entropy of the protein environment with the decrease of the entropy in the solvent environment (Table II). The P3 changes from F to small hydrophobic (A), polar neutral (S) and charge residues (K^+) reduces the affinity of the PlmII for the substrate because the enthalpy penalty ($\Delta\Delta H$) is higher than the raise in the entropy ($T\Delta\Delta S$) of the system (Table III). However, the raise in the entropy ($T\Delta\Delta S$) of these mutations have different basis. In the case of the change from ($F \rightarrow K^+$) the raise in the entropy of the complex environment

To further explore the enthalpy diff in binding between the P3 mutants, we extract the enthalpic and entropic contribution from the binding free energy diff. We did this for PlmII, all F mutation using the finite

analyze diff. enthalpic effect. Explain clearer. Maybe histogram plot. This is too dry. too much higher, lower etc.

prevails over the raise in the entropy of the solvent environment. In the case of the change from ($F \rightarrow A$) the entropy penalty ($T\Delta S$) in the solvent environment is higher than in the protein environment. Conversely, the raise in the entropy of the change from ($F \rightarrow S$) is the combination of the raise of the entropy in the protein environment with the decrease in the solvent environment. On the other hand, the P3 change from ($F \rightarrow D^0$) reduce the affinity of PlmII for the substrate due to the entropy penalty ($T\Delta\Delta S$) overcomes the decrease in the enthalpy ($\Delta\Delta H$) of the system. Additionally, we have to remark that the entropy penalty ($T\Delta\Delta S$) in this mutation is the consequence of the drop off in the entropy of the protein environment.

To get a better understanding of the changes in the entropy of these systems due to the environment reorganization effects caused by the mutations in the P3 position of the substrate, we calculated the configurational entropy contributions ($T\Delta\Delta S^{conf}$, Table IV) to the binding entropy differences. It should be noted the relationship between the raise in the entropy of the environment reorganization ($T\Delta\Delta S - T\Delta\Delta S^{conf}$) with the increase of the bulky of the side chain mutated ($F \rightarrow K^+ \approx F \rightarrow I > F \rightarrow S > F \rightarrow A$). However, we observed that the entropy penalty of the P3 change from ($F \rightarrow D^0$) is determined by the entropy penalty of the environment reorganization effects.

incomplete.
maybe
ignore
at all, beca
calculations
of S^{conf}
have very
large spread
($S^{conf}_{complex}$ for
F)

Discussion

Understanding the PlmII S3 subsite preference

Understanding the specificity differences between PlmII and the human aspartic proteases is a useful requirement for designing specific inhibitors that will interact with the parasite protein and not with the human counterparts. Here, we studied the PlmII S3 subsite pocket preference by non-equilibrium free energy calculations using the CGI method. Earlier kinetic experiments indicated the major role of this subsite pocket in the PlmII specificity.²⁸ Our calculations showed that the P3 changes from hydrophobic residues (F, I or A) to neutral polar (S), acid (D⁰) or charged residues (K⁺, and R) decrease the affinity of Plasmepsin II for the substrate. This fit well with the experimental trend of relative binding free energy differences between PlmII:Substrate complexes obtained from Westling *et al* (Table II, Figure 3).²⁸ These authors found that PlmII prefers large hydrophobic residues within the S3 subsite pocket, while lysine or aspartic acid substitutions in P3 were not well tolerated.²⁸ Interestingly, we observed that the substrate P3 position was always solvent exposed in the PlmII:Substrate complexes. A previous study demonstrated the significant better accuracy of the CGI method for calculating the free energy change due to amino acid substitutions for surface residues (78.4% within ± 4.18 kJ/mol of experimental values) than for core residues (65.5%).³⁹

Should the same calculations be performed for Cat D? To analyse selectivity.

implication.

why here. That is already discussed in vitro.

We predicted that the lysine and aspartic acid residues in the substrate P3 position must be in the protonated form in the experimental assays carried out at pH = 4.4.

So do explain.

Relate this literature back to our observation

This prediction allowed explaining: i) the 2.5-fold decrease in K_m of the PlmII M15E mutant for a substrate with D in the P3 position with respect to the wild-type protein, and ii) the 7-fold decrease in K_m of this mutant for a substrate with K in P3 with respect to the wild-type protein.²⁸ These results demonstrated that the M15 residue contributes to the S3 subsite specificity of PlmII.²⁸ In addition, the M15E mutant data support the theory that the presence of a Glu at this position in aspartic proteinases enhances the binding of substrates/inhibitors with Lys in P3.^{40, 41} Furthermore, because PlmII differs at position 15 from the human enzymes: cathepsin D, cathepsin E, and pepsin,²⁶ specific inhibitors may be rationally designed to take advantage of this specificity distinction.²⁸

highlight M15 in Figure 1

what is different

~~Despite~~ Previous studies indicated that PlmII has a stringent requirement for hydrophobic amino acid in the P3 position of peptide substrates.^{28; 42, 43} It was demonstrated that the PlmII M15E mutant processes a hemoglobin-based substrate that contains an Arg in the P3 position, with an equal efficiency as the wild-type enzyme.²⁸

Is this efficiency high or low

Gulnik *et al* observed a similar behavior for the wild-type enzyme with another substrate containing Arg in the P3 position.⁴⁴ These authors suggested that the preference of PlmII for certain amino acids in particular subsites may depend strongly on the substrate sequence context.⁴⁴ On the other hand, our ^{calculation} predictions indicated a ^{for rege} higher decrease in the PlmII affinity for the change in the P3 position from $F \rightarrow R$ than from $F \rightarrow K^+$. This agreed well with the experimental data obtained by Beyer *et al.*⁴³

implication. Relation to previous.

Despite the limitations, the synthetic peptide combinatorial libraries have been widely used to determine the substrate preference of the Pf DV Plms.^{27, 43} However, these approaches can not elucidate the thermodynamic origin of the low tolerance for the acid or basic residues within the PlmII S3 subsite. Here, we showed the different basis of the relative binding free energy differences due to the ^{mutations} changes in the substrate P3 position.

what are these results?

It should be remarked that the unfavorable effect of the change from $F \rightarrow D^0$ over the PlmII:Substrate complex affinity is the consequence of the lower favorable effect of this mutation on the bound state than in the unbound state. In the case of the change from $F \rightarrow R$ the decrease in the Plasmepsin II affinity is the combination of an unfavorable effect in the complex with a favorable effect in the solvent system. Conversely, the change from $F \rightarrow K^+$ reduces the affinity of PlmII for the substrate due to the higher unfavorable effect of this mutation on the complex system than in the solvent system (Table II). This results indicated that to improve the affinity of PlmII inhibitors is wished: i) mutations more favorable on the complex state than in the solvent state, ii) mutations less unfavorable on the complex state than in the solvent state, or ideally iii) mutations more favorable on the complex state and more unfavorable on the solvent state.

what about deprotonation in the solvent

Is there any other way? Which mutations result in one of these states. Is there a general rule?

What can we learn for PlmII inhibitor design?

Designing more potent ligands to a known receptor needs to consider how to introduce new functional groups in the ligand structure that improve the transfer process of the ligand from the solution (free state) into the binding site of the solvated receptor (bound state). The binding affinity of a compound can be improved by generating a favorable binding enthalpy, favorable solvation entropy, or by minimizing the unfavorable conformational entropy.⁴⁵ It should be remarked that extremely high affinity is achieved when the three factors are optimized simultaneously.

Earlier thermodynamic studies of PlmII with several inhibitors, derived from the allophenylnorstatine scaffold, and ranging in the nM K_i affinities, revealed that the

Be careful, this is ΔS ^{of binding} and we have calculated $\Delta \Delta S$ of binding and ΔS of mutation

entropic contribution is the dominant driving force for binding.¹¹ According to our calculations the change from $F \rightarrow I$ is the only one that increases the affinity ($\Delta \Delta G$) of PlmII for the substrate due to the higher unfavorable effect of this mutation in the unbound state than in the bound state. At the thermodynamic level the binding affinity is determined by the magnitude of the Gibbs energy (ΔG), an additive function ($\Delta G = \Delta H - T\Delta S$) of the enthalpy (ΔH) and entropy changes (ΔS).⁴⁶ The analysis of the entropy and enthalpic contributions of the change from $F \rightarrow I$ showed that this mutation is an entropy driven process because the raise in the entropy ($T\Delta \Delta S$) prevails over the enthalpy penalty ($\Delta \Delta H$). It should be remarked that the binding entropy is defined by two major terms, the first one is the solvation entropy associated with the burial from the solvent of hydrophobic groups, and the second one is the conformational entropy, which usually reflects the loss of conformational degrees upon binding.⁴⁶ Based on our results the raise in the entropy of the environment reorganization ($T\Delta \Delta S - T\Delta \Delta S^{conf}$) due to the change from $F \rightarrow I$ overcomes the loss of the conformational degrees upon binding of this side chain mutation.

there is no process, because these mutations do not occur naturally.

not really because $\Delta \Delta G = -0.11 \pm 1.38$. So the energy gain is much smaller than the error.

very inaccurate.

From the engineering point of view, a favorable enthalpy change is obtained from good geometric complementarities between drug and target, ^{Also} and the proper location of hydrogen bond donors and acceptors is an important contributor to the drug affinity and selectivity.⁴⁵ The structural analysis of the PlmII:Substrate complexes indicated that the hydroxyl group of the Tyr side chain in the P3 position interacts with the solvent and not with the PlmII S3 subsite pocket residues. This allowed explaining our prediction of the null effect over the PlmII:Substrate affinity from the change $F \rightarrow Y$. This suggested the high degree of difficulty associated to optimize the enthalpy contributions of PlmII peptidomimetic inhibitors by introducing polar groups in the P3 position.

Other than that the interactions are the same.

Isn't that simply because it is a hydrophobic pocket.

Concluding remarks

In this paper, we found that the CGI method can be suitably applied to study the binding free energy differences of substitutions in the substrate P3 position over the PlmII:Substrate complexes affinities. We focused on the study of the PlmII S3 substrate preference considering previous kinetic experiments which suggested the major role of this subsite pocket in the protease specificity. Our results agreed well with the relative experimental trend of relative binding free energy differences from these systems, and allowed explaining the energetic basis of low tolerance of PlmII S3 subsite pocket by the lysine and aspartic acid residues in the substrate P3 position. This fit well with previous works that describe the highly hydrophobic character of this subsite pocket.

The structural analysis of the PlmII:Substrate complexes showed that the substrate P3 position is solvent exposed. This suggested the high degree of difficulty to optimize the enthalpy contribution of PlmII peptidomimetic inhibitors by the introduction of polar groups in P3.

Additionally, we predicted that the lysine and aspartic acid residues in the P3 position of the substrate must be in the protonated form in the experimental assays.

Methods

Comparative 3D Modeling

Three dimensional models for PlmII:Substrate complexes were generated with the MODELLER software,⁴⁷ using as template the crystallography structure of PlmII complexed with a peptide-based inhibitor (PDB code: 2r9b, R = 2.8 Å). We calculated 20 models for each complex with the spatial restraints extracted from the target-template alignment. These models were assessed using the UCLA web server tools (<http://nihserver.mbi.ucla.edu/SAVS/>); and the DOPE energy function⁴⁸ provided with the modeling package.⁴⁷ *No simulations to test stability?*

Alchemy free energy calculations

We calculated relative binding free energy differences for 22 point mutations in the P3 positions of PlmII:Substrates complexes (K-P-X-E-F*Nph-R-L, where Nph = para-nitrophenylalanine, * indicates the cleavage point, and X the amino acid variation in P3).²⁸ Each mutation was automatically setup with the PYMACS package (<http://www.user.gwdg.de/~dseelig/pymacs.html>), a collection of scripts which, 1) replace residues in the structure file by the appropriate mutation, and 2) modify the GROMACS topology files to ensure the correct force field parameters for each state.³⁹ All Molecular Dynamics (MD) simulations were carried out using the GROMACS software package (version 4.0.7)⁴⁹ with the AMBER99sb force field⁵⁰, and the TIP3P water model⁵¹. As simulation protocol, we chose non-equilibrium fast-growth thermodynamic integration (FGTI) runs. For determining the $\Delta\Delta G$ binding value of each PlmII:Substrate P3 mutation, equilibrium ensembles at $\lambda=0$ and at $\lambda=1$ are required for the bound and unbound states. The bound simulation systems consist of the complex solvated in a dodecahedron box with ≈ 14192 water molecules and NaCl was added to achieve a 100 mM solution. The unbound simulation systems consist of the substrate solvated in a similar box with ≈ 3193 water molecules and 100 mM of NaCl. Both the A- and B-states were sampled for 100 ns using the stochastic dynamic integrator at 310 K and constant pressure of 1 atm using the Parrinello-Rahman barostat.⁵² The electrostatic interactions were calculated at every step with the particle-mesh Ewald method^{53, 54}, and short-range repulsive and attractive dispersion interactions simultaneously described by a Lennard-Jones potential with a cutoff of 1.1 nm and a switching function that was used between 1.0 and 1.1 nm. Dispersion correction for energy and pressure was applied. The SETTLE⁵⁵ algorithm was used to constrain bonds

and angles of water molecules., and LINCS ⁵⁶ was used for all other bonds, allowing a time step of 2 fs.

From these ensembles, the first 2 ns were discarded, 196 snapshots were taken, and short simulations were performed in which λ was changed from zero to one, respectively. For the FGTI simulations, we used the leap-frog integrator⁵⁷ with the velocity rescaling thermostat. ⁵⁸ Energy calculations, timestep, and pressure coupling were setup analogous to the equilibrium runs. To account the occurrence of atomic overlaps close to $\lambda = 0$ and $\lambda = 1$, soft-core potentials were used for both electrostatics and Lennard-Jones interactions as implemented in GROMACS-4.0 with $\alpha = 0.3$, $\sigma = 0.25$, and a soft-core power of 1. The complete switching from $\lambda = 0$ to $\lambda = 1$ was done within 100 ps and the derivatives of the Hamiltonian with respect to λ were recorded at every step. Free energies were calculated from the work distribution obtained from integration according to:

$$W = \int_{\lambda=0}^{\lambda=1} \frac{\partial H_{\lambda}}{\partial \lambda} d\lambda \quad [1]$$

and calculating the intersection of the forward and backward work distributions according to the Crooks-Gaussian-intersection method previously described. ³⁸ Binding free energy differences $\Delta\Delta G = \Delta G_3 - \Delta G_2 = \Delta G_4 - \Delta G_1$, were calculated from the difference of the free energies between the bound (complex) and unbound (substrate) mutation simulations according to the thermodynamic cycle shown in the Figure 2.

Experimental binding free energies differences ($\Delta\Delta G_{exp}$) of each P3 mutation in PlmII:Substrates complexes were calculated from the experimental Michaelis constant values (Km) ²⁸ at 310 K considering that:

$$\Delta\Delta G_{exp} = RT \times \ln \left(\frac{Km_B}{Km_A} \right). \quad [2]$$

To measure the overall fit between $\Delta\Delta G_{exp}$ and $\Delta\Delta G_{calc}$, we calculated the Pearson product-moment correlation coefficient (r) using equation 3:

$$r_{xy} = \frac{n \sum x_i y_i - \sum x_i \sum y_i}{\sqrt{n \sum x_i^2 - (\sum x_i)^2} \sqrt{n \sum y_i^2 - (\sum y_i)^2}} \quad [3]$$

where n is the sample size, and x_i and y_i are the $\Delta\Delta G_{exp}$, and the $\Delta\Delta G_{calc}$ values for each P3 mutation, respectively.

How did you treat the mutation that involve charge diff.

Entropy and enthalpy calculations

The constant-pressure binding entropy differences ΔS (310K, 1 atm) were obtained from the finite difference relationship:

$$\Delta S(T) = -\frac{\Delta G(T + \Delta T) - \Delta G(T - \Delta T)}{2\Delta T} \quad [4]$$

where we used $\Delta T = 25$ K. The binding free energies $\Delta G(T + \Delta T)$ and $\Delta G(T - \Delta T)$ were calculated according the thermodynamic cycle shown in Figure 2. The constant-pressure binding enthalpy was calculated according to the equation 5:

$$\Delta G = \Delta H - T\Delta S \quad [5]$$

The configurational binding entropy differences ΔS^{conf} (310K, 1 atm) from the equilibration MD runs of the bound and unbound states were estimated based on the use of the quasiharmonic analysis with the covariance related to the quantum-mechanical entropy formula.⁵⁹

Binding Interaction analyses

We calculated the heavy atom-atom contacts between the P3 residue of the substrate and the binding site residues using 0.4 nm as distance cutoff criteria along the MD trajectories. We considered as stable contacts pair each one, we a frequency (f) $f \geq \frac{1}{m}$, where m is the mean contact per atom. Then, we calculated the fraction of non-polar/polar contacts for each P3 residue of the substrate with the S3 subsite residues of the protein.

Acknowledgements

PAV acknowledges the DAAD and EMBO financial support for performing a research stay in the Max Planck Institute of Biophysical Chemistry, Göttingen, Germany.

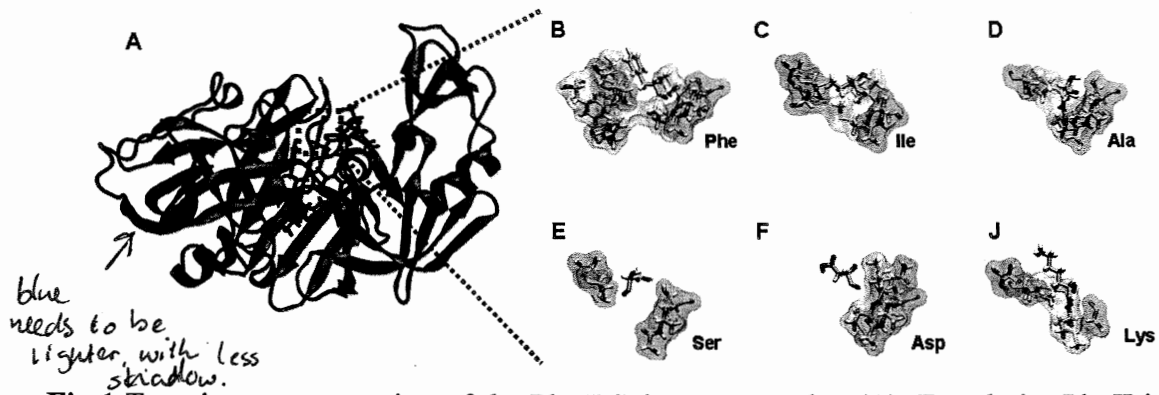


Fig 1 Top view representation of the PlmII:Substrate complex (A). For clarity PlmII is represented as a blue cartoon diagram, and the substrate as a red licorice diagram. The black box highlighted the substrate P3 position. Surface side view representation of the interaction between the PlmII S3 subsite residues and different amino acids in the substrate P3 position: B) Phe, C) Ile, D) Ala, E) Ser, F) Asp, and J) Lys. For clarity the substrate P3 position is represented as a licorice diagram, and the non polar residues in the PlmII S3 subsite pocket were displayed as gray, while the polar residues were displayed as green.

Why does the size of the pocket change ~~between~~ in A-J
 Maybe place waters as lines in A-J

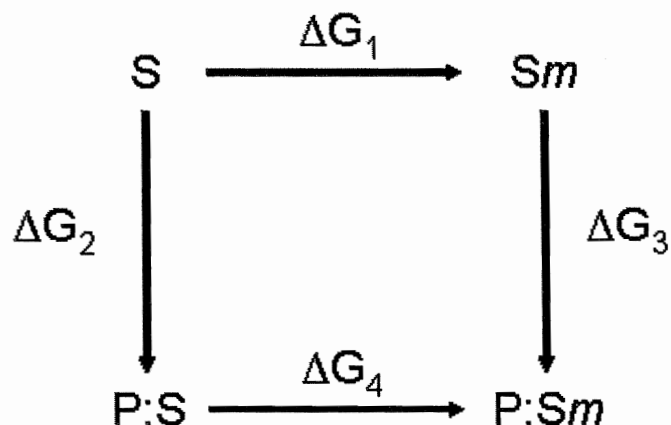


Fig 2 Thermodynamic cycle for the free energy calculations. S and Sm represented the state A and state B from of the substrate in solution, respectively. P:S and P:Sm represented the state A and state B of the PlmII:Substrate complex, respectively. The binding free energy differences $\Delta\Delta G = \Delta G_3 - \Delta G_2$ for the amino acid variations in the substrate P3 position of the PlmII:Substrate complexes can be calculated via $\Delta\Delta G = \Delta G_4 - \Delta G_1$.

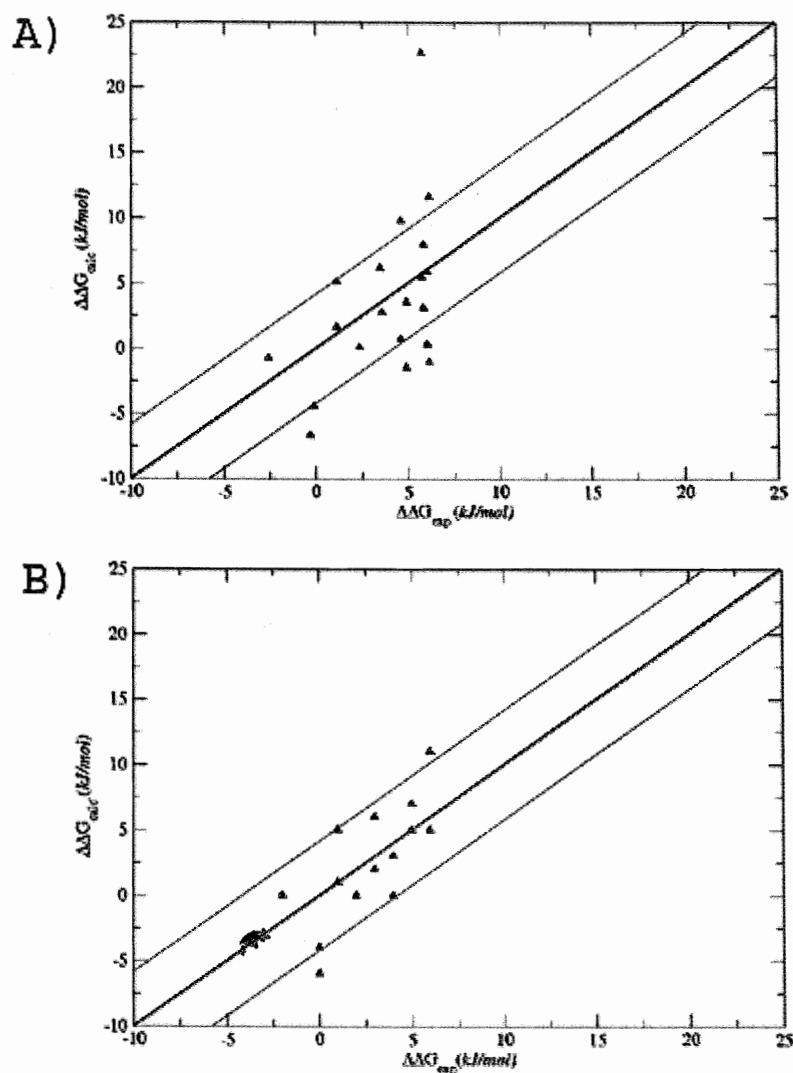


Fig 3 Scatter diagram of calculated ($\Delta\Delta G_{\text{calc}}$) versus experimental ($\Delta\Delta G_{\text{exp}}$) binding free energy differences of PlmII:Substrate complexes using the CGI method. The two red lines parallel to the diagonal line represent deviations of ± 4.18 kJ/mol. (A). Calculated binding free energy differences in the P3 positions of PlmII:Substrates complexes considering both protonation of the ionizable residues. (B) Calculated binding free energy differences in the P3 positions of PlmII:Substrates complexes considering the protonation of the ionizable residues that fit better with experimental results.

Table I Summary of the atomic interactions differences between the substrate P3 position and the P1mII S3 subsite contact residues

P3 residue	Fraction Non Polar	Fraction Polar	Km (μM) ^a
<i>F</i>	0.65	0.35	24 \pm 3
<i>I</i>	0.47	0.53	23 \pm 3
<i>A</i>	0.27	0.73	37 \pm 8
<i>S</i>	0.38	0.62	92 \pm 9
<i>K</i>	0.56	0.44	250 \pm 60
<i>D</i>	0.60	0.40	221 \pm 57

a) The experimental Km values were taken from reference 28.

Table II Calculated and experimental binding free energy differences of mutations in the substrate P3 position of PlmII-Substrates complexes.

P3 Mutations (A → B)		$\Delta G_{complex}^a$ (kJ/mol)	$\Delta G_{substrate}^b$ (kJ/mol)	$\Delta \Delta G_{calc}^c$ (kJ/mol)	$\Delta \Delta G_{exp}^d$ (kJ/mol)	error ^e (kJ/mol)
F → A		30.01 ± 0.42	28.40 ± 0.25	1.61 ± 0.49	1.12	0.49
F → S		-21.29 ± 0.48	-27.43 ± 0.35	6.14 ± 0.59	3.47	2.67
F → I		8.94 ± 0.50	13.43 ± 0.30	-4.49 ± 0.59	-0.11	4.38
F → K	K ⁺	688.56 ± 1.08	682.72 ± 0.62	5.84 ± 1.25	6.04	0.20
	K ⁰	-59.24 ± 1.54	-59.55 ± 0.95	0.31 ± 1.81		5.73
F → D	D ⁻	-1239.38 ± 1.29	-1261.97 ± 0.76	22.59 ± 1.49	5.74	16.85
	D ⁰	-213.29 ± 0.60	-218.75 ± 0.30	5.48 ± 0.67		0.26
F → R		3.37 ± 1.57	-4.12 ± 0.73	7.49 ± 1.73	-	-
F → Y		-101.27 ± 0.29	-101.26 ± 0.18	-0.01 ± 0.34	-	-
I → A		25.26 ± 0.43	20.21 ± 0.20	5.05 ± 0.47	1.11	3.94
I → S		-28.87 ± 0.52	-31.60 ± 0.24	2.73 ± 0.57	3.57	0.84
I → K	K ⁺	681.70 ± 1.02	670.14 ± 0.46	11.56 ± 1.57	6.15	5.41
	K ⁰	-74.29 ± 1.09	-73.20 ± 0.64	-1.09 ± 1.26		7.24
I → D	D ⁻	-1268.14 ± 1.10	-1271.23 ± 0.96	3.09 ± 1.46	5.83	2.74
	D ⁰	-219.01 ± 0.63	-226.93 ± 0.40	7.92 ± 0.75		2.09
A → S		-53.82 ± 0.22	-53.86 ± 0.14	0.04 ± 0.27	2.35	2.31
A → K	K ⁺	657.05 ± 0.71	653.51 ± 0.47	3.54 ± 0.85	4.92	1.38
	K ⁰	-90.83 ± 0.86	-89.37 ± 0.63	-1.46 ± 1.06		6.38
A → D	D ⁻	-1280.59 ± 0.79	-1290.33 ± 0.88	9.74 ± 1.18	4.61	5.13
	D ⁰	-246.20 ± 0.40	-246.89 ± 0.33	0.69 ± 0.52		3.92
(K) → S		-882.43 ± 0.78	-881.55 ± 0.58	-0.78 ± 0.97	-2.57	1.79
(K) → D	D ⁻	-	-	-	-0.32	-
	D ⁰	-1080.42 ± 1.03	-1073.73 ± 0.74	-6.69 ± 1.27		6.37

protonation
state
normally
R⁺ pKa(12.5)

ΔG too
small for
charge
introduction.

u⁺, u⁰?

a) $\Delta G_{complex}^a$ of each P3 mutations in the PlmII-substrate complexes were obtained with the CGI method.

b) $\Delta G_{substrate}^b$ of each P3 mutations in the substrate-solvent systems were obtained with the CGI method

c) Calculated binding free energy differences ($\Delta \Delta G_{calc}^c$) of each P3 mutation in the systems were calculated using the relationship $\Delta \Delta G_{calc} = \Delta G_{complex} - \Delta G_{substrate}$

d) Experimental binding free energy differences ($\Delta \Delta G_{exp}$) of each P3 mutation in PlmII-substrates complexes at 310 K was calculated using the relationship $\Delta \Delta G_{exp} = RT \times \ln \left(\frac{Km_B}{Km_A} \right)$. The experimental

Michaelis constant values (Km) of each complex were taken from ref. 28.

e) Absolute error|error| refer to deviations, in kJ/mol, between the calculated and experimental values of each P3 mutation in the PlmII-substrate complexes.

Table SI Calculated binding free energy differences of mutations in the PlmII substrate P3 position at 335 and 285 K

P3 mutations (A → B)	$\Delta G_{335K}^{complex}$ (kJ/mol)	$\Delta G_{335K}^{substrate}$ (kJ/mol)	$\Delta\Delta G_{335K}$ (kJ/mol)	$\Delta G_{285K}^{complex}$ (kJ/mol)	$\Delta G_{285K}^{substrate}$ (kJ/mol)	$\Delta\Delta G_{285K}$ (kJ/mol)
$F \rightarrow A$	30.28 ± 0.38	30.47 ± 0.24	-0.19 ± 0.45	29.23 ± 0.46	28.47 ± 0.24	0.76 ± 0.52
$F \rightarrow S$	-25.60 ± 0.57	-25.63 ± 0.28	-0.03 ± 0.64	-23.89 ± 0.54	-26.39 ± 0.54	2.5 ± 0.62
$F \rightarrow I$	12.14 ± 0.56	12.35 ± 0.29	-0.21 ± 0.63	13.36 ± 0.42	11.19 ± 0.36	2.17 ± 0.55
$F \rightarrow K^+$	684.65 ± 1.13	679.26 ± 0.62	5.39 ± 1.31	692.71 ± 1.11	686.07 ± 0.93	6.64 ± 1.45
$F \rightarrow D^0$	-213.04 ± 0.40	-220.20 ± 0.46	7.16 ± 0.61	-218.05 ± 0.63	-220.12 ± 0.38	2.07 ± 0.74

I remember discussing with Pedro that there was some inaccuracy problem in these calculations.

→ That was configurational entropy